



ELSEVIER

Physica B 298 (2001) 369–375

PHYSICA B

www.elsevier.com/locate/physb

Optical spectroscopy of magnetic 2D electron gases at the Los Alamos pulsed magnetic field facility

S.A. Crooker^{a,*}, D.G. Rickel^a, E. Johnston-Halperin^b, D.D. Awschalom^b,
R. Knobel^c, N. Samarth^c, S.K. Lyo^d, A. Efros^e

^aNational High Magnetic Field Laboratory, Los Alamos National Laboratory, MS E536, Los Alamos, NM 87545, USA

^bDepartment of Physics, University of California, Santa Barbara, CA 93106, USA

^cDepartment of Physics, Pennsylvania State University, University Park, PA 16802, USA

^dSandia National Laboratory, P.O. Box 5800, MS-1415, Albuquerque, NM 87185, USA

^eNanostructure Optics Section, Naval Research Laboratory, Washington, DC 20375, USA

Abstract

A brief overview of the magnet technologies at the pulsed field facility at Los Alamos is presented, focusing on the experimental capabilities made possible by the unique generator-driven 60 T long-pulse magnet. Optical spectroscopy is one such beneficiary, and recent measurements of semiconductor systems are discussed, including studies of magnetic-disorder annealing in diluted magnetic semiconductors, “dark” excitons in CdSe quantum dots, and in particular, studies of negatively-charged exciton states in magnetic 2D electron gases. Here, the huge Zeeman energy inherent in these magnetically-doped II–VI materials results in a completely spin-polarized electron gas (even at low magnetic fields), and drives an apparent instability of the singlet (spin antiparallel) electrons that are bound to the photohole. © 2001 Elsevier Science B.V. All rights reserved.

Keywords: Pulsed magnetic fields; Charged excitons; Quantum dots; Magnetic semiconductors

1. Los Alamos pulsed field facility – overview

The primary focus of the NHMFL pulsed magnetic field facility in Los Alamos is to provide state-of-the-art pulsed magnet technology and support infrastructure for both in-house researchers as well as for the international scientific community. In particular, the NHMFL-pulsed field facility offers a wide range of capacitor-driven “short-pulse” magnets (50–60 T peak field, 25–100 ms pulse dura-

tion) and “mid-pulse” magnets (40–50 T, ~600 ms pulse duration), in addition to the flagship generator-driven 60 T long-pulse magnet (2000 ms pulse duration) which features a user-definable field profile. The high-resolution spectroscopic studies to be discussed in this paper were largely enabled by the long-pulse magnet.

In August/September of 1999, the laboratory was relocated to an entirely new and significantly upgraded experimental hall (Fig. 1), incorporating specifically redesigned control software and switching hardware to enable parallel operation of multiple pulsed magnet experiments. Six short-pulse magnet stations may be automatically switched to

* Corresponding author. Fax: +1-505-665-4311.
E-mail address: crooker@lanl.gov (S.A. Crooker).

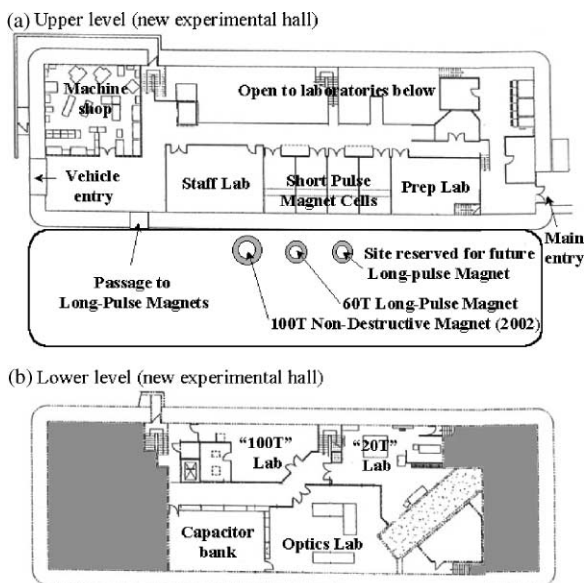


Fig. 1. Layout of the new experimental hall at the NHMFL pulsed field facility.

a common, fast-charging 1.6 MJ capacitor bank, so that all experiments operate independently. The 60 T long-pulse magnet is located in an adjoining building and runs independently of the short-pulse magnets. The long-pulse magnet is powered by a 1.4 GVA motor-generator and five 84 MVA pulse-shaping power supplies which drive the magnet once per hour, making this the most powerful controlled-pulse magnet system in the world [1]. At the time of writing, the 60 T long-pulse magnet has delivered nearly 1000 shots since its completion in 1998. Magnet pits also exist for the 100 T non-destructive magnet, which is scheduled for completion in 2002 and will incorporate both generator- and capacitor-driven technologies [2].

Low temperature magneto-transport and magnetization (dHvA) measurements are particularly well suited to the short-pulse magnets, as recent studies in the high T_c superconductor $\text{Bi}_2\text{Sr}_{2-x}\text{La}_x\text{CuO}_{6+\delta}$ [3], and heavy fermion alloys $\text{La}_{1-x}\text{Ce}_x\text{B}_6$ [4] demonstrate.

The very long (2 s) pulse duration of the 60 T long-pulse magnet, combined with the capability to tailor the field profile, makes a number of new experimental techniques possible in pulsed mag-

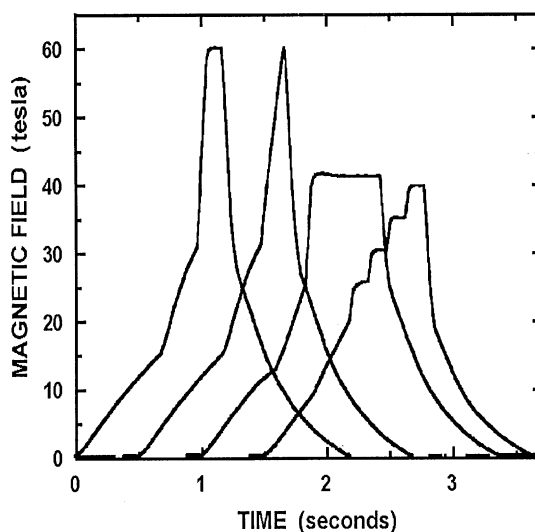


Fig. 2. Sample field profiles for the 60 T long-pulse magnet, user selectable from pulse to pulse based on the needs of the particular experiment.

netic fields. The choice of field profile is essentially limited only by the maximum ramp rates and total thermal loading of the magnet. Fig. 2 shows four of the more common field profiles selected for experiments. The first is the canonical 60 T ‘flat-top’ pulse, where 60 T is maintained for a full 100 ms and the field is ramped up and down at the maximum rate. Second is the ‘stretched-ramp’ profile, which minimizes dB/dt during the upswing and is used for most spectroscopic studies, where up to 2000 optical spectra are collected throughout the entire magnet pulse [5–7]. Next is a flat-top at 40 T (or any other field), where the field is held constant at a particular value for as long as possible—this field profile has proven especially useful for high-field studies of time-resolved photoluminescence, to gather the maximum number of photons at fixed field. Last is the ‘stairstep’ profile, which provides the opportunity to collect data at several different field values in a single magnet pulse. The capability to provide ‘flat-top’ and ‘stairstep’ field profiles has enabled unprecedented heat-capacity measurements in pulsed magnets. Here, Jaime et al. [8] measured the Sommerfeld coefficient (the ratio C/T as $T \rightarrow 0$) of the Kondo insulator $\text{Ce}_3\text{Bi}_4\text{Pt}_3$ to 60 T, which shows an abrupt rise at ~ 40 T

indicating a field-driven closure of the Kondo energy gap. The 60 T LP magnet has also enabled sensitive measurements of the low-temperature *c*-axis magneto-transport in the optimally doped high- T_c superconductor $\text{Bi}_2\text{Sr}_2\text{CaCu}_2\text{O}_{8+\delta}$, where Morozov et al. [9] established a negative magnetoresistance at high fields in support of interlayer quasiparticle tunneling in a d-wave superconductor.

2. Pulsed-field optical spectroscopies of semiconductors

The 60 T long-pulse magnet affords, in conjunction with a high-speed CCD camera, ample time to acquire many high-resolution optical spectra throughout a single magnet pulse. For typical studies of photoluminescence (PL), absorption or reflection, spectra are acquired every 1 to 2 ms during both the up-sweep and down-sweep of the pulse, so that the entire field-dependence may be reconstructed and checked for consistency. Similar methods are also applied in the 40 and 50 T mid-pulse capacitor-driven magnets, with slightly reduced field resolution. Here, we present three different spectroscopic studies of semiconductor nanostructures in pulsed fields.

2.1. Field-driven annealing of magnetic disorder in diluted magnetic semiconductor quantum wells

Here, pulsed magnetic fields to 60 T are used to drive an annealing of the *microscopic magnetic disorder potential* in an alloyed semiconductor. This annealing is directly revealed through the linewidth of the exciton PL [5]. Unlike nonmagnetic alloyed semiconductors (e.g., $\text{Al}_{1-x}\text{Ga}_x\text{As}$) which exhibit a fixed alloy fluctuation potential, the microscopic disorder in diluted magnetic semiconductors (e.g., $\text{Zn}_{1-x}\text{Mn}_x\text{Se}$) is sensitive to the applied field, offering a field-tunable system in which to test existing theories of compositional disorder. This sensitivity arises, via the $J_{s\text{-pd}}$ exchange interaction, from the strong dependence of the local bandgap near a Mn^{2+} cation on the Mn^{2+} spin orientation. In these $\text{Zn}_{1-x-y}\text{Cd}_x\text{Mn}_y\text{Se}$ quantum wells, Mn^{2+} spins which are aligned by the magnetic field reduce

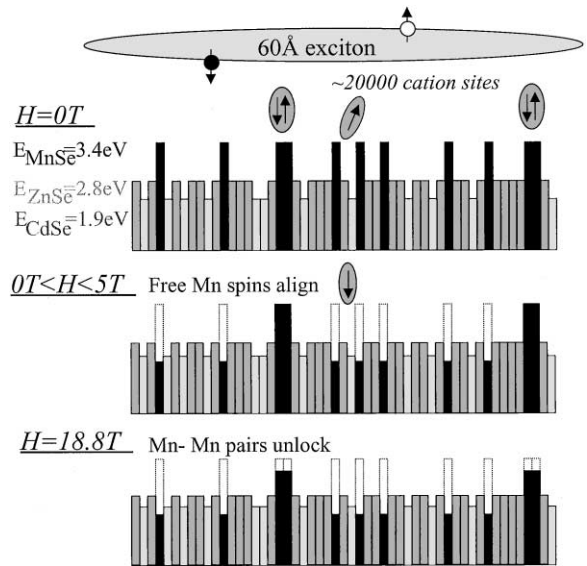


Fig. 3. The magnetic annealing process, wherein high fields lower the local bandgap near Mn^{2+} ions, reducing the total rms alloy disorder as seen by an exciton.

the local bandgap near the Mn^{2+} cation site, thus lowering the net rms alloy fluctuation seen by the ensemble of recombining excitons, and decreasing the total PL linewidth (see Fig. 3). The data reveal a rapid drop in linewidth at low fields ($H < 8\text{ T}$) as single Mn^{2+} spins are aligned. At higher fields, antiferro-magnetically bound Mn–Mn pairs partially unlock, giving rise to clear steps in the magnetization and further drops in the alloy disorder, measured directly through the PL linewidth (Fig. 4). Existing theories of alloy disorder reproduce the general shape of the linewidth annealing, but markedly underestimate the magnitude of the effect.

2.2. Spin-spectroscopy of ‘dark excitons’ in CdSe quantum dots

Chemically synthesized CdSe nanocrystallites are a particularly well-studied class of semiconductor quantum dot (QD). It is thought that the 0-D confinement in these QDs leads to a huge electron–hole exchange interaction, which in turn generates a pronounced exciton fine structure wherein the ground state is a nominally ‘dark’

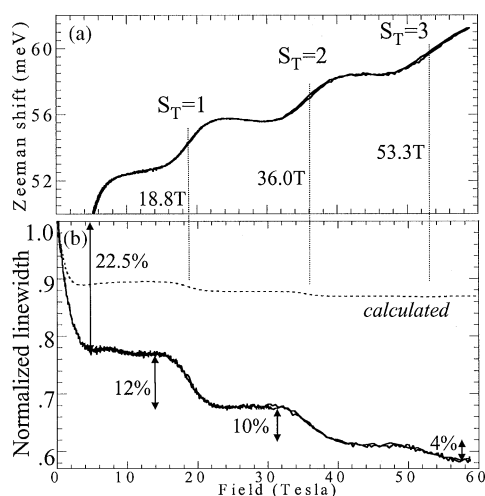


Fig. 4. (a) Magnetization of the sample, proportional to the energy shift of the exciton PL. Steps at high fields arise from unlocking of Mn–Mn pairs. (b) The corresponding PL linewidth, showing sharp drops at magnetization steps.

($J = 2$) exciton [10]. Little is known about the spin structure of this state, although it is predicted that magnetic fields will admix the dark excitons with the higher-lying ‘bright’ ($J = 1$) excitons, permitting a direct, optically allowed transition of the dark exciton. High fields are required to approach the intrinsic meV-scale exchange splittings between dark and bright excitons, and to this end we investigate the degree of PL polarization from CdSe QDs in fields to 60 T [11]. The data reveal a significant degree of circular polarization which exhibits an unusual high-field behavior (Fig. 5). At low temperatures, the polarization rolls off near 20 T at a value of only ~ 0.6 (well below full 100% saturation), and increases only slowly thereafter to the highest fields.

Fig. 5c shows the degree of polarization dropping rapidly with increasing temperature, reminiscent of the behavior expected of a thermal ensemble of optically active excitons distributed between two Zeeman-split spin states. Further, time- and polarization-resolved studies reveal that the degree of circular polarization remains nearly constant throughout the decay (Fig. 6), verifying a thermal ensemble of excitons. Based on these findings we develop a model of the PL emission from the $J = 2$ dark excitons, which accounts for the random ori-

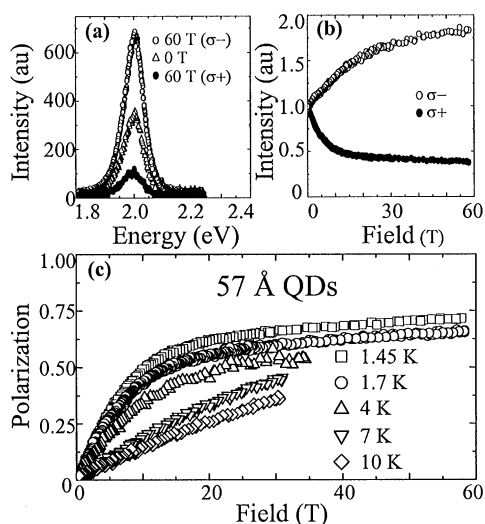


Fig. 5. Circularly polarized PL from CdSe quantum dots. (a) Raw spectra, (b) intensities, and (c) polarization to 60 T.

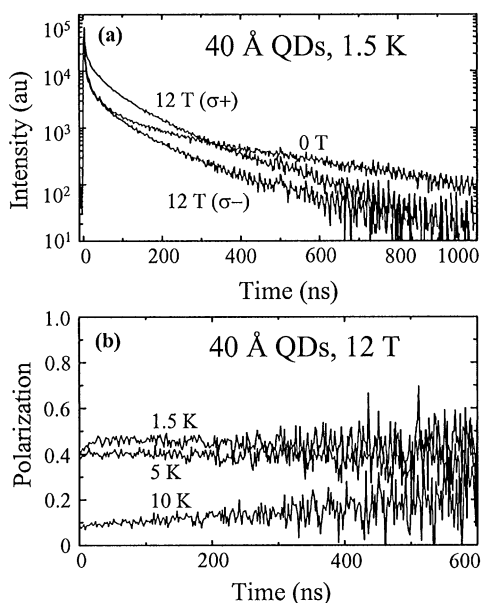


Fig. 6. (a) Time- and polarization-resolved PL from CdSe QDs at 0 and 12 T. (b) Time-resolved polarization at 12 T, indicating a thermal ensemble of dark excitons.

entation of the QDs with respect to the applied field. The shape (slightly prolate) and crystal (wurtzite) anisotropy of the QDs presents a strongly preferred c -axis along which spin angular

momentum is quantized. Thus, only magnetic fields parallel to the c -axis induce a Zeeman splitting of the $J = 2$ dark excitons, whereas fields orthogonal to c admix the bright and dark exciton states as theoretically predicted in Ref. [10]. Thus, the sample consists of an ensemble of QDs with varying Zeeman splittings and varying admixtures of bright and dark excitons. The predicted polarization is found to exhibit precisely the observed behavior—an initial saturation at 0.625 when the field-induced mixing is low, growing slowly with field to 0.75, which is the maximum polarization possible from an ensemble of randomly oriented wurtzite QDs.

2.3. Stability of trions in spin-polarized magnetic 2D electron gases

Magnetic two-dimensional electrons gases (2DEGs) represent a relatively new class of

semiconductor quantum structure in which an electron gas is made to interact strongly with embedded local moments. They are typically realized in doped II–VI diluted magnetic semiconductor quantum wells wherein paramagnetic spins (Mn^{2+} , $S = 5/2$) interact with the confined electrons via the strong J_{s-d} exchange interaction. This interaction leads to a greatly enhanced spin splitting (10–20 meV) of the electron Landau levels. This Zeeman energy can exceed both the cyclotron and Fermi energies at low fields, resulting in a 2DEG having entirely spin-polarized Landau levels.

This investigation [6] focused on the properties of negatively charged excitons (two electrons bound to a single hole) in these spin-polarized 2DEGs. The singlet state of the negatively charged exciton (X_s^- trion) is the ground state of a low-density electron gas at zero magnetic field. However, the spin anti-parallel nature of the electrons in X_s^- suggests that the stability of this singlet state

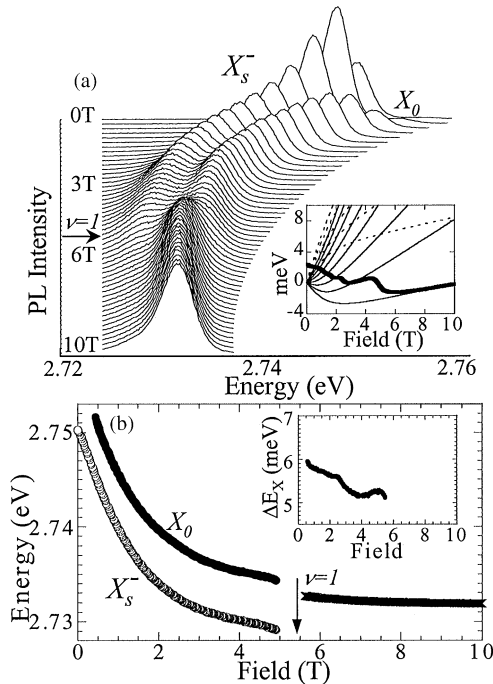


Fig. 7. (a) PL spectra and calculated chemical potential (inset) at 1.5 K for a magnetic 2DEG ($n_e = 1.2 \times 10^{11} \text{ cm}^{-2}$). (b) Energies of the PL peaks. Inset: the X_s^- ionization energy, which mimics the chemical potential.

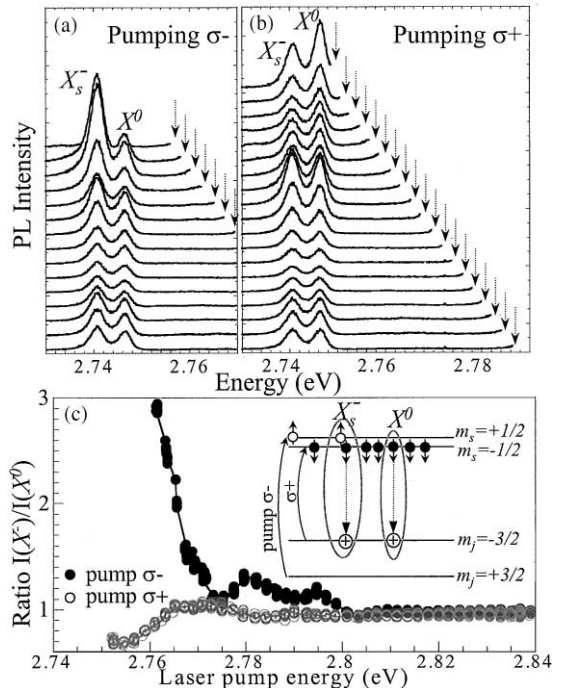


Fig. 8. (a,b) PL excitation at 2.2 K and 1 T, showing an enhancement of X_s^- (X_0) when injecting spin-up (down) electrons at the σ^- (σ^+) resonance. (c) The X_s^-/X_0 intensity ratio, with schematic of the energy levels.

must depend on the Zeeman energy and spin polarization of the 2DEG.

Fig. 7a shows the PL from a low-density magnetic 2DEG with increasing field. Two peaks exist at low fields which we associate with X_s^- and the neutral exciton X^0 . The Landau levels and calculated chemical potential for this sample are shown in the inset, where solid (dotted) lines correspond to spin-down (up) levels. The energy between these PL peaks is the X_s^- ionization energy (Fig. 7b, inset), which mimics the chemical potential. At $\nu = 1$ the spectra collapse and are replaced by a single PL peak which persists to 60 T.

Fig. 8 verifies the assignment of the X_s^- and X^0 features in PL by selectively and resonantly photo-exciting electrons of particular spin orientation into the 2DEG. Here, resonant excitation with $\sigma -$ light increases the population of spin-up electrons and thus the probability of X_s^- formation, as diagrammed in Fig. 8c. In contrast, excitation with $\sigma +$ light can (and does) only increase the formation of X^0 . Thus the PL of Fig. 7a may be understood as follows: X_s^- and X^0 are competing channels for exciton formation, with X_s^- domina-

ting at zero field. With small applied field, the large spin splitting drives a rapid depopulation of the spin-up electron bands, reducing the probability of X_s^- formation and enhancing X^0 formation, as observed. With increasing field and Zeeman energy, X_s^- continues to form, with reduced binding energy, until it is no longer energetically favorable to bind a spin-up electron – in this case, evidently, when the Fermi energy falls to the lowest Landau level. The PL peak which emerges at $\nu = 1$ with an energy between that of X_s^- and X^0 is likely the spin *triplet* state of the negatively charged exciton (X_t^-), with spin-parallel electrons. X_t^- , which must be the only stable trion in the limit of infinite Zeeman energy, may be forming stably in these spin-polarized magnetic 2DEGs due to the large Zeeman energy.

The surprising degree to which the X_s^- ionization energy (ΔE_X) seems to mimic the chemical potential of the 2DEG is demonstrated in Fig. 9, which shows the measured ΔE_X along with the calculated chemical potential below. Aside from a ~ 7 meV absolute difference in energy, which is associated with the ‘bare’ X_s^- binding energy, the similarity is striking regardless of either electron density or

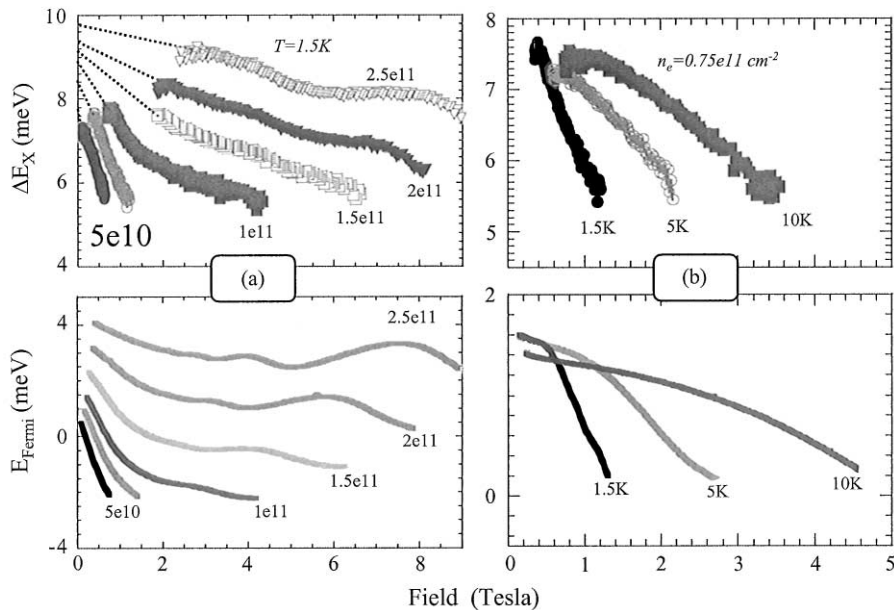


Fig. 9. (a) Measured X_s^- ionization energy for magnetic 2DEGs with different density, with calculated chemical potential below. (b) Same, for different temperatures.

temperature. At least at zero field, the data are consistent with a suggested scenario [12] in which ΔE_x equals the ‘bare’ binding energy plus the Fermi energy (i.e., the energy required to remove one electron from X_s^- and place it at the top of the Fermi sea). However, with applied field the large Zeeman energy plays a critical role, reducing ΔE_x until X_s^- destabilizes. In particular, the oscillations observed in Fig. 9a and especially the apparent roll-off of ΔE_x towards zero field in Fig. 9b suggest that the energy *between* the Fermi energy and the lowest spin-up subband plays a critical role. These experiments complement similar pulsed-field studies [13,14] of charged excitons in nonmagnetic III–V 2DEGs, also performed at the NHMFL-pulsed field facility.

Acknowledgements

S.A.C. would like to especially thank J. Schillig, M. Gordon, and M. Pacheco for their help and

expertise. Experiments performed at the National High Magnetic Field Laboratory are supported by the US National Science Foundation through Cooperative Grant No. DMR 9016241, the State of Florida, and the US Department of Energy.

References

- [1] J. Schillig et al., IEEE Trans. Appl. Superconductivity 10 (2000) 526.
- [2] J. Sims et al., IEEE Trans. Appl. Superconductivity 10 (2000) 510.
- [3] S. Ono et al., Phys. Rev. Lett. 85 (2000) 638.
- [4] R. Goodrich et al., Phys. Rev. Lett. 82 (1999) 3669.
- [5] S.A. Crooker et al., Phys. Rev. B 60 (1999) R2173.
- [6] S.A. Crooker et al., Phys. Rev. B 61 (2000) R16307.
- [7] S.A. Crooker et al., Phys. Rev. B 61 (2000) 1736.
- [8] M. Jaime et al., Nature 405 (2000) 160.
- [9] N. Morozov et al., Phys. Rev. Lett. 84 (2000) 1784.
- [10] Al. Efros et al., Phys. Rev. B 54 (1996) 4843.
- [11] E. Johnston-Halperin et al., Phys. Rev. B, to be published.
- [12] V. Huard et al., Phys. Rev. Lett. 84 (2000) 187.
- [13] F. Munteanu et al., Phys. Rev. B 61 (2000) 4731.
- [14] Y. Kim et al., Phys. Rev. B 61 (2000) 4492.